Environ. Sci. Technol. **2005**, *39,* 6170−6181

Relating Desorption and Biodegradation of Phenanthrene to SOM Structure Characterized by Quantitative Pyrolysis GC-MS

NAOKO WATANABE,[†]
EGBERT SCHWARTZ,[‡,§]
KATE M. SCOW,[‡] AND
THOMAS M. YOUNG*,[†]
Department of Civil and Environmental Engineering and Department of Land, Air, and Water Resources, University of California, Davis, One Shields Avenue, Davis, California 95616

A set of four soils was extensively studied for composition, sorption/desorption, and biodegradation to investigate linkages among these three inter-related factors. Composition of soil organic matter (SOM) was quantitatively characterized using pyrolysis GC-MS; although CO_2 dominated the total ion chromatogram for all soils, each soil produced a distinctively different pyrogram and 1.4−4.8% of the soil carbon was quantified as one of 205 pyrolysis marker compounds using external standards. Amorphous and free iron and aluminum contents were determined as potential indicators of the reactivity of the mineral phase, which may influence the configuration and accessibility of SOM domains within soil. We observed a statistically significant positive correlation between two-site model fast fraction *f* values derived from mineralization and desorption rate studies, which suggests that desorption limits biodegradation. However, no statistically significant correlation was observed between two-site model fast and slow rate constants (k_f, k_s) for the two processes. No evidently strong correlations were found between functional parameters (organic carbon normalized distribution coefficient K_{OC}, hyeteresis index *HI*, and two-site model parameters *f*, k_f, and k_s for both desorption and biodegradation and maximum rate and extent of biodegradation) and SOM structural descriptors (pyrolysis results). Lack of strong correlations may suggest (i) that multiple SOM structures are collectively responsible for desorption resistance or (ii) that the pyrolysis GC-MS method used in this study was unable to identify relevant structures. In contrast, amorphous and free iron and aluminum contents showed statistically significant correlations with K_{OC} and *HI* values, indicating the potential importance of underlying mineral phases in determining desorption and biodegradation rates.

Introduction

Many organic contaminants become sequestered as they age in soil and sediment. Sequestered organic compounds often resist desorption (*1*, *2*), extraction (*3*, *4*), and biodegradation (*3*, *5*−*8*) and may pose lower toxicity (*3*, *9*, *10*). Understanding the reasons for resistance to desorption and biodegradation is of great importance in predicting the fate and transport of contaminants as well as in accurately assessing their risks. Soil and groundwater contamination are often addressed using bioremediation or natural attenuation and both methods typically depend on the ability of microorganisms to rapidly degrade the pollutant.

Contaminant fate is determined by synergistic interactions among three system features: (1) soil/sediment characteristics, (2) sorption/desorption processes, and (3) biodegradation. There are numerous studies about the relation between soil/sediment characteristics and sorption/desorption processes (*11*, *12*). Rate-limited sorption has been explained by two major hypotheses: (i) slow diffusion within the soil organic matter (SOM) matrix or in nanopores within organic matter or in soil minerals or (ii) sorption to high-energy sites within molecular size voids (*11*, *13*) or in molecular size pores (*14*, *15*) or on high surface area carbonaceous materials (*16*, *17*). SOM is highly heterogeneous and has regions with different rigidity (*18*, *19*). Rubbery or expanded regimes provide linear, rapidly reversible partitioning, and glassy or condensed regimes cause nonlinear, slowly reversible or irreversible sorption. Soot- or charcoal-like carbonaceous materials (collectively termed black carbon) in soils and sediments show strong sorptive capacities (*20*−*22*). Isotherm nonlinearity, hysteresis, and desorption resistance have been correlated to various organic matter features including polarity (*23*), aromaticity (*24*, *25*), aliphaticity (*26*), black carbon or soot content (*20*), and degree of diagenesis (*27*, *28*). The effects of mineral-organic matter complexation on sorption properties have also been studied, but to a lesser extent (*29*−*31*). Although several indicators have been suggested for correlating sorption behavior with soil characteristics, none so far seems to work universally for all types of soils and sediments.

The relationship between desorption and biodegradation has also been the focus of extensive study (*32*). Bioavailability often appears to be limited by desorption resistance, especially in weathered samples. The limiting effects of the presence of soil on biodegradation rates and the comparability of desorption and biodegradation rates have been widely documented. (*5*, *33*−*35*) Ogram et al. (*36*) found that biotransformation of the herbicide 2,4-dichlorophenoxyacetic acid in the presence of soil was explained best by a model that assumed that adhered and suspended bacteria were able to degrade the compound only in solution, whereas the sorbed compound was protected from biodegradation. Scow and Hutson (*37*) showed that biodegradation of organic compounds increasingly deviated from first-order kinetics and were better described by double-exponential decay curves with increasing sorbent content or diffusion path length. Alvarez-Cohen et al. (*38*) found that in the presence of silicalite the rate of trichloroethylene (TCE) biotransformation was proportional to the solution-phase TCE concentration and was independent of the mass in the sorbed phase.

However, some evidence indicates certain bacteria may have an ability to mineralize sorbed compounds. Possible mechanisms include excretion of metabolites that facilitate desorption and direct utilization of compounds by microorganisms that adhere to the same surface (*39*). Tang et al. (*40*) showed that a mixed culture and a pure isolate obtained by enrichment on sorbed phenanthrene readily degraded phenanthrene sorbed to the beads or sediment, and the rate

* Corresponding author phone: (530)754-9399; e-mail: tyoung@ucdavis.edu.
[†] Department of Civil and Environmental Engineering.
[‡] Department of Land, Air, and Water Resources.
[§] Present address: Department of Biological Sciences, Northern Arizona University, Flagstaff, Arizona, 86011-5640.

10.1021/es0480522 CCC: $30.25

Published on Web 07/16/2005

TABLE 1. Characteristics of Soils Studied

soil	OC %	N %	C/N	sand/silt/clay %	pH[a]	CEC meq/ 100 g[a]	moisture retention (0.333 bar) %	free mg/g OC		amorphous mg/g OC		soil classification
								Fe	Al	Fe	Al	
Forbes	4.30	0.19	22.6	33.5/44.1/22.4	5.6	14.0	40.3[a]	4464	462	110	287	fine, oxidic, mesic, ultic palexeralf
Tinker	11.0	0.49	22. 4	78.0/17.2/4.8	4.8	20.8	41.6[a]	196	140	37.8	93.4	loamyskeltal, mixed, mesic, typic durumbrept
Yolo Surface	1.20	0.14	8.6	19.9/57.4/22.7	7.0	n.a.[c]	23.2[b]	3738	409	152	60.0	fine-silty, mixed nonacid, thermic, typic xerothent
Yolo Vadose	0.32	0.04	8.0	19.5/56.0/24.5	n.a.	n.a.	21.1[b]	11 675	1406	869	250	Vadose zone soil (1.5 m deep), agricultural, CA

[a] Reference *46*. [b] Reference *47*. [c] n.a.: not available.

of mineralization was faster than the rate of desorption in sterile systems. Guerin and Boyd (*41*, *42*) tested two bacterial species for their ability to mineralize naphthalene in soils and demonstrated that while one species could only mineralize naphthalene in aqueous phase, the other was capable of degrading sorbed naphthalene.

There are few studies relating SOM characteristics to biodegradation. SOM characteristics can be important, especially when microorganisms utilize sorbed compounds either by excretion of enzymes/surfactants or by adhesion to the surface that enables them to directly contact the sorbed molecules. White et al. (*8*) found no evident relationships between bioavailability and organic matter contents, clay contents, or aggregate size distributions. Guerin and Boyd (*41*, *42*) found no obvious correlation between biodegradation (initial rate, final extent) and organic matter properties (organic carbon (OC) content, OC normalized distribution coefficient (K_{OC}), and the aromaticity of humic acid extracted from the soil). Tang et al. (*43*) showed that bacteria and earthworms have different rates and extents of uptake of aged compounds from soil indicating that desorption is not the only factor that controls bioavailability.

The purpose of this study is to explore relationships among soil characteristics, sorption/desorption properties, and the rate and extent of biodegradation. The goal is to use SOM characteristics and desorption properties as determinants to understand variations in the rate and extent of biodegradation between soils. It is challenging to establish such relationships unambiguously with reasonable sample numbers since soil is a complex mixture of heterogeneous organic and mineral matter supporting a diverse microbial population. To provide insight into these processes, sorption/desorption phase distribution relationships (PDRs) and the rate and extent of both desorption and mineralization were measured for four soil samples. Soil organic matter was characterized using quantitative pyrolysis GC-MS. Amorphous and free iron and aluminum contents were also determined because these were hypothesized to influence the configuration and accessibility of SOM domains to sorbates.

Materials and Methods

Soil Properties. All of the experiments used four California soils. Forbes soil was collected from a conifer and oak forest in the Tahoe National Forest, Placer County, CA, and Tinker soil was collected from a mixed coniferous forest in the Tahoe National Forest, Nevada County, CA. Yolo Surface and Yolo Vadose soils were collected from an organic farm at the University of California, Davis. Soil fractions passing through a 2-mm sieve were stored in sealed bags at 4 °C and were maintained at field moisture level for mineralization experiments and at room temperature for other experiments. Free and amorphous aluminum and iron contents were determined using published procedures (*44*, *45*). The properties of the soils are summarized in Table 1.

Pyrolysis GC-MS. A detailed description of the quantitative pyrolysis GC-MS method is provided in Watanabe and Young (unpublished manuscript). A brief description of these methods follows. Soil samples (5−20 mg) were weighed into quartz tubes, heated to 650 °C at a rate of 10 °C ms^{-1}, and held at this temperature for 30 s in He using a pyrolyzer (AS 2000, CDS Analytical, Oxford, PA). The organic matter that volatilized was analyzed by a GC-MS (HP GCD 5890, Hewlett-Packard, Palo Alto, CA) following separation in a capillary column (ZB-5, 30 m × 0.25 mm i.d. and 0.25-μm film thickness, Phenomenex, Torrance, CA). The He flow was 1 mL/min. The initial temperature of 35 °C was held for 5 min followed by heating to 280 °C at 10 °C/min which was held for 20 min. The amount of organic matter that was pyrolyzed was quantified by subtracting the weights of the pyrolysis residues from the weights of the samples. The top 50 peaks in total ion counts from each soil during preliminary pyrolysis analysis were combined to make a list of compounds for quantification. From this list, 155 compounds were selected as external standards on the basis of commercial availability; standard curves for these compounds were generated for selected ions by direct injection using the above GC-MS method. A standard curve for carbon dioxide was generated by introducing a known volume of carbon dioxide from a Tedlar bag. Using the standard curves, 205 compounds were quantified. There are more quantified compounds than standard curves because response factors for some of the standards were also applied to quantify other fragments of similar structures such as series of alkanes, alkenes, and alkyl substituted benzenes. Each soil sample was analyzed in triplicate and the results were averaged.

Phase Distribution Relationships. Bottle point phenanthrene adsorption and desorption PDRs were measured using 40-mL glass centrifuge tubes with Teflon-lined caps. A PDR describes the distribution of a solute between solvent and sorbent phases at a particular contact time; if the system attains equilibrium, the PDR is equivalent to an isotherm (*48*, *49*). Target masses for each sorbent were Forbes 100 mg, Tinker 200 mg, Yolo Surface 800 mg, and Yolo Vadose 800 mg. Soil masses were chosen so that 40−95% of the phenanthrene is sorbed at the selected contact time of 1 week. A 1-week sorption time was used because the majority of sorption typically occurs in 1 week and PDR parameters across soils and sediments at a fixed contact time are strongly correlated with the corresponding isotherm parameters on the basis of previous rate studies (*49*, *50*). Aqueous phenanthrene solution was buffered with 0.0018 M $NaHCO_3$, and 0.015 M $CaCl_2$ was used as a background electrolyte, and 0.005 M NaN_3 was added to control microbial activity. Ten different initial concentrations were prepared (2.5−750 μg/L) in triplicate, and a blank control containing no soil was prepared at each initial concentration. The samples were tumbled end-over-end at room temperature (23 ± 1 °C). The tubes were then centrifuged at 2000 rpm for 20 min, and the supernatant was decanted and analyzed. After weighing the

tubes to allow the mass of phenanthrene discarded from the system to be calculated, buffer solution containing no phenanthrene was added to the tubes and the samples were tumbled for 1 week at room temperature to determine desorption PDRs. The tubes were centrifuged and the supernatant was analyzed. Sorbed phase concentrations were calculated by difference. Average system losses determined from blank controls were 5.3% of the initial solute concentration indicating that sorption to tubes and Teflon-lined caps was negligible.

Phenanthrene concentrations in the supernatant were analyzed using HPLC (1100 Series, Hewlett-Packard, Palo Alto, CA) equipped with 5 μm ODS-3 column (100 × 2.0 mm, Phenomenex, Torrance, CA) with either a diode array detector at 250 nm or 291 nm or a fluorescence detector with an excitation wavelength of 250 nm and an emission wavelength of 364 nm. An isocratic 90/10 acetonitrile/water mixture was used at a flow rate of 0.2 mL/min with a sample injection volume of 5 μL.

Desorption Rate Studies. Desorption rates of phenanthrene from the soils into completely mixed aqueous slurries were measured. Soils were γ-irradiated with ^{60}Co irradiation at 355 299 rad/hr for 14.083 h at the Nuclear Reactor Laboratory, University of Michigan, prior to the experiments (*51*). Soils were returned to a moisture content of 0.222 bar with autoclaved milli Q water containing 0.005 M NaN_3 and were kept at 25 °C for 1 month, then spiked with phenanthrene in dichloromethane, and mixed with a sterilized spatula for 5 min and in a tumbler for 25 min, and then the solvent was allowed to evaporate for 30 min. The same spiking procedure was used for the mineralization studies (*52*). Soil samples were then capped and stored in the dark at 25 °C for periods from 1 day to 18 months. The term "aging" is used in the remainder of the article to refer to phenanthrene contact time with the soils prior to the initiation of desorption or biodegradation experiments. Solid-phase phenanthrene concentrations were targeted to be at equilibrium with 250 μg/L aqueous phase concentration from the PDRs: Forbes 160 μg/g, Tinker 400 μg/g, Yolo Surface 48 μg/g, and Yolo Vadose 24 μg/g. Desorption rates were measured in triplicate. Spiked soil (0.6 g), water (40 mL), and Tenax TA (60/80) beads (0.2 g) were continuously mixed in 50-mL Teflon centrifuge tubes in a tumbler. Tenax beads have been used as a sink for hydrophobic compounds in previous work (*2*, *53*). At designated times, the tubes were centrifuged to separate the Tenax beads, which float at a moderate centrifuge speed, from the soil suspension. Clean Tenax beads were placed in the centrifuge tubes and the tubes were returned to the tumbler. The Tenax beads separated from the suspension were extracted in 1-butanol, which was analyzed using HPLC. A phenanthrene isotherm in the Tenax/1-butanol system was measured prior to the experiment, and the amount of phenanthrene remaining with the Tenax after extraction was calculated and added to the amount measured in the 1-butanol extract. Tenax beads lowered the aqueous phase concentration from 500 μg/L to below 6 μg/L in less than 5 min when the phenanthrene loading to the beads was below 70 μg/g, which was achieved throughout the experiment.

Desorption rate experiments were carried out for up to 18 months, and the final sorbed phase concentrations were determined by Soxhlet extracting freeze-dried soil samples at the conclusion of the desorption experiment. The mass of phenanthrene recovered in blank Soxhlet extractions including no soil was 0.03 (±0.03) μg/extraction and counted for less than 0.7% of the mass extracted from the soil samples. To confirm that there was no significant residual phenanthrene on soil samples after 24 h of Soxhlet extraction with methanol, an additional Soxhlet extraction with hexane/acetone (50/50) was performed after extended hours (72 h) of methanol extraction for 1-week-aged Forbes and Tinker soils following aqueous desorption. Neither extended hours of methanol extraction nor extraction with hexane/acetone yielded significant amounts of additional phenanthrene. The contributions of the additional extractions to the measured residual concentrations were less than 8% for Forbes soil and 6% for Tinker soil, which were less than the standard deviations of the measured residual concentrations.

TABLE 2. Pyrolysis Recoveries

	OM recovery %[a]	OC recovery %[b]	OC recovery without CO_2 %[c]	N recovery %[d]
Forbes	83.3 (2.6)[e]	90.9 (0.9)	3.7 (0.6)	17.7 (3.3)
Tinker	46.9 (9.3)	69.4 (4.8)	4.8 (0.2)	10.9 (1.7)
Yolo Surface	98.7 (5.2)	65.4 (20.1)	3.1 (1.1)	8.7 (2.7)
Yolo Vadose	138.1 (10.4)	75.2 (7.1)	1.4 (0.3)	3.2 (0.3)

[a] OM recovery = soil mass pyrolyzed (μg) × 100%/{soil OM content (%) × 0.01 × mass of the soil sample (μg)}. [b] OC recovery = [Σ (moles of quantified compund × number of carbon in the compound)] × 12 × 10^6 (μg/mole) × 100%/{soil OC content (%)/soil OM content (%) × soil mass pyrolyzed (μg)}. [c] OC recovery without CO_2 = OC recovery (b) − OC recovery as CO_2. [d] N recovery = [Σ (moles of quantified compund × number of nitrogen in the compound)] × 14 × 10^6 (μg/mole) × 100%/{soil N content (%)/soil OM content (%) × soil mass pyrolyzed (μg)}. [e] () shows standard deviation.

Desorption rate curves were plotted by adding each Tenax-extracted increment to the final sorbed concentrations. The recoveries of phenanthrene computed as the sum of the final Soxhlet result and all Tenax increments compared to the initial solid-phase loading determined by Soxhlet extraction were Forbes 90.0% (±9.9%), Tinker 86.3% (±9.8%), Yolo Surface 100.5% (±19.6%), and Yolo Vadose 94.3% (±4.3%) with numbers in parentheses showing standard deviations.

Mineralization Studies. Mineralization studies were performed in soils with a moisture content of 0.222 bar. Soils were inoculated with Arthrobacter strain RP17, which can use phenanthrene as its sole carbon and energy source and mineralize it to CO_2 (*51*). A mixture of ^{14}C labeled (Sigma Chemical Co., St Louis MO, >98% purity, specific activity of 59 mCi/mmol) and nonisotopically labeled phenanthrene was added to 20 g dry weight soil in 100 μL of dichloromethane at 50 ng/g. Phenanthrene was mixed into the soil with a spatula by hand for 2 min. After the designated aging time, RP17 was added to the soil at 1.2 × 10^8 cfu/g and the soil was incubated at 28 °C in an airtight pint mason jar with a trap containing 1 mL of 0.5 N NaOH. Three replicate samples were prepared for each soil. The base was periodically sampled, and its radioactivity was measured in a liquid scintillation counter (Beckman Instruments, Inc., Fullerton, CA). The mason jar was opened during sampling to ensure sufficient oxygen remained available over the course of the incubation. Details about the method and about the RP17 inoculum are further described in Schwartz and Scow (*54*) and in Schwartz et al. (*52*).

Results and Discussion

Pyrolysis GC-MS. A detailed analysis of the quantitative pyrolysis GC-MS results is contained in Watanabe and Young (unpublished manuscript). Pyrolysis recoveries are summarized as OM, OC, and N recoveries (Table 2). OM recovery is calculated as the mass fraction pyrolyzed with respect to the OM content of each soil. OC recovery is determined by comparing the carbon mass of all quantified pyrolysis fragments to the mass of OC contained in the soil pyrolyzed. Similarly, the N recovery is calculated by comparing the mass of N contained in all quantified pyrolysis fragments to the N content of the soil pyrolyzed. Forbes and Tinker soils, which have higher OM contents, showed lower OM recoveries. This may be caused by char-forming reactions that compete with the pyrolysis process. OC was recovered predominantly as CO_2; OC recovery without CO_2 ranged from 1.4% (Yolo

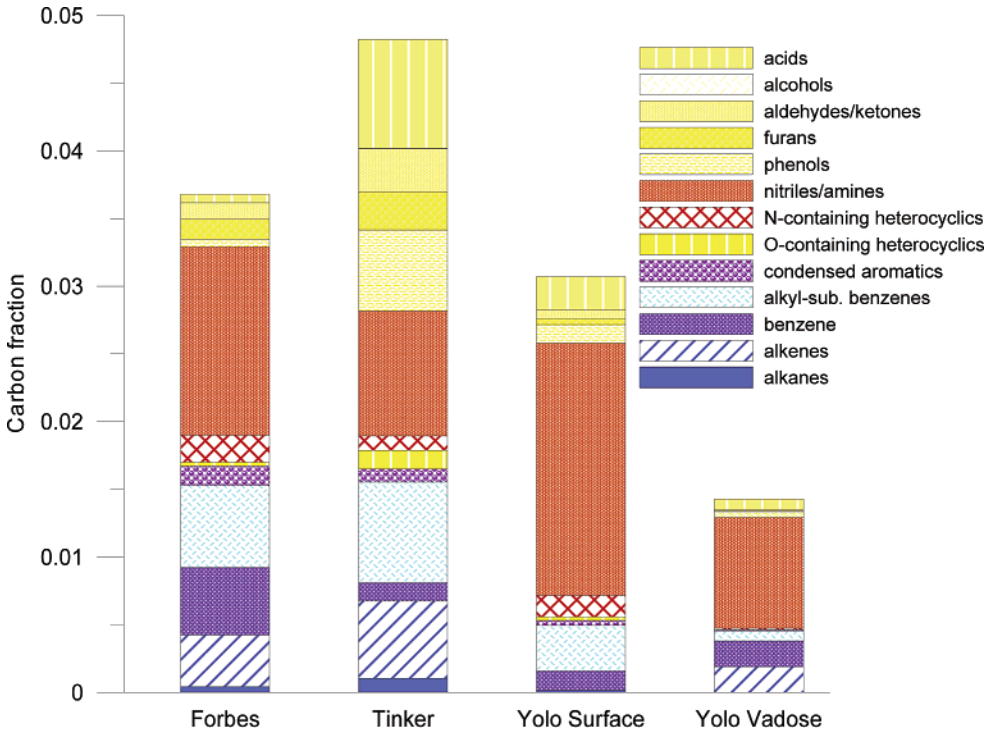

FIGURE 1. Pyrolysis results. Carbon fractions of 205 quantified compounds summed over 14 structural groups. Representative compounds in each group include alkanes: *n*-octane to *n*-tritriacontane, alkenes: 1-hexene to 1-octacosene, alkyne: 2,4-hexadiyne; benzene: benzene; alkyl-substituted benzenes: toluene to phenylicosan, styrene, 1,2,4-trimethylbenzene; condensed aromatics: naphthalene, phenanthrene, pyrene, chrysene, indene, methylindene; O-containing heterocyclics: 1,6-anhydro-beta-D-glucopyranose, 2-furaldehyde; N-containing heterocyclics: pyrrole, *N*-methylpyrrole, pyridine, 3-picoline, isoquinoline, 2-methylbenzoxazole; nitriles/amines: acetonitrile, aniline, benzonitrile, *m*-tolunitrile, phenylacetonitrile; phenols: phenol, 4-methylphenol, 2-methoxyphenol, 2-methoxy-4-methylphenol, 2,6-dimethoxyphenol; furans: 2-methylfuran, 5-methylfurfural, benzofuran, dibenzofuran; aldehydes/ketones: acetaldehyde, acetone, 2-methyl-2-cyclopenten-1-one, isovanillin, acetovanillone; alcohols: allyl alcohol, benzyl alcohol; acids: acetic acid, tetradecanoic acid. No detectable alkynes were observed.

Vadose) to 4.8% (Tinker). N recovery was also low, between 3.2% (Yolo Vadose) and 17.7% (Forbes). Possible reasons for N and C recoveries below 100% include volatilization of pyrolysis products or formation of polar or high molecular weight pyrolysis products that are not suitable for GC-MS analysis. The recoveries were also incomplete because there were hundreds more pyrolysis fragments that were not quantified. For nitrogen, unquantified compounds include nitrogen gas, ammonia, and oxides of nitrogen. No observable ammonia peak was present in the pyrograms, possibly because it was not adequately resolved from the large water peak.

Although CO_2 was easily the largest peak in the total ion chromatogram for all soils, each soil produced a distinctively different pyrogram (Figure S1 and Table S2 in Supporting Information), which presumably reflects differences in original SOM structures. To facilitate subsequent correlation analysis, carbon fractions of the 205 quantified compounds were summed over the 14 structural groups shown in Figure 1. Forbes produced the greatest fraction of benzene, condensed aromatics, and N-containing heterocyclics. Tinker produced more O-containing groups than any other soil such as O-containing heterocyclics, phenols, furans, aldehydes/ketones, and acids. The nitriles/amines group was dominant in Forbes, Yolo Surface, and Yolo Vadose. Although the total carbon fraction quantified for Yolo Vadose was half of that of Yolo Surface over the 14 groups, their composition was similar. Yolo Vadose produced more alkenes and benzene and fewer alkanes, O-containing heterocyclics, and furans than Yolo Surface. This agrees with the SOM changes expected to occur in a depth profile (*55*).

Principal component analysis of the pyrolysis data was performed to analyze the relationships among the 14 structural groups and among the soil samples (Figure 2). Each axis is a weighted composite of the 14 structural groups, and the arrows show where a particular structural group falls in the space defined by the first two principal components. Component one, which accounts for 57.8% of the variation in the data set, is the overlap of hydrocarbons (alkanes, alkenes, and alkyl substituted benzenes) and

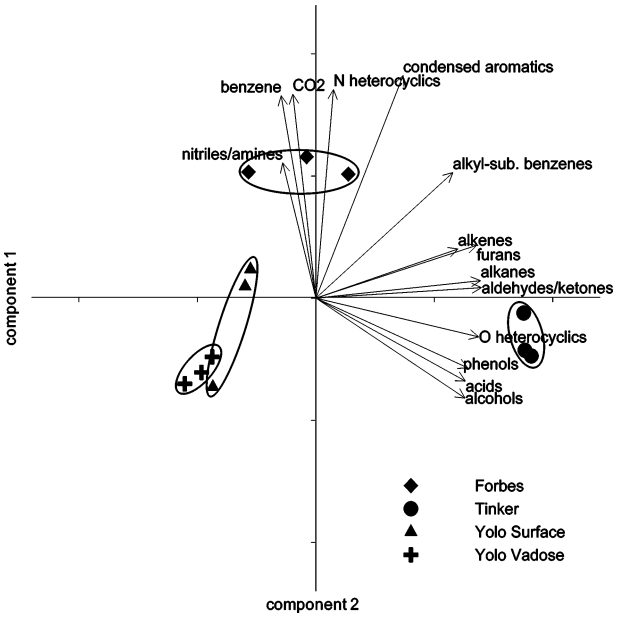

FIGURE 2. Principal component analysis of the pyrolysis results summed over 14 structural groups.

TABLE 3. Sorption and Desorption PDR Parameters

soil	process	Log K_F[a]	n[a]	R^2	N[b]	aqueous concn range (μg/L)	K_{OC}[c] (L/g)	HI[d]
Forbes	sorption	0.045 (0.019)	0.86 (0.012)	0.99 5	30	0.54−329	13.4	0.69
	desorption	0.25 (0.019)	0.87 (0.015)	0.99 2	30	0.26−135	22.7	
Tinker	sorption	0.58 (0.027)	0.86 (0.023)	0.98 5	23	0.44−85.6	18.1	0.080
	desorption	0.68 (0.020)	0.83 (0.019)	0.98 9	23	0.31−65.7	19.6	
Yolo Surface	sorption	−0.26 (0.0093)	0.78 (0.0071)	0.99 8	24	0.45−147	16.7	0.082
	desorption	−0.092 (0.0096)	0.71 (0.0080)	0.99 7	24	0.24−91.2	18.1	
Yolo Vadose	sorption	−0.58 (0.021)	0.72 (0.013)	0.99 3	24	1.52−331	22.8	0.75
	desorption	−0.44 (0.025)	0.77 (0.020)	0.98 6	24	0.98−93.7	39.8	

[a] () shows standard deviation. [b] N: number of data points. [c] Organic carbon normalized distribution coefficients $K_{OC} = 100 \cdot K_D/OC\% = K_F C_e^{(n-1)}$ at $C_e = 100$ (μg/L). [d] Hysteresis index $HI = (q_e(\text{desorption}) - q_e(\text{sorption}))/q_e(\text{sorption})$ at $C_e = 100$ (μg/L).

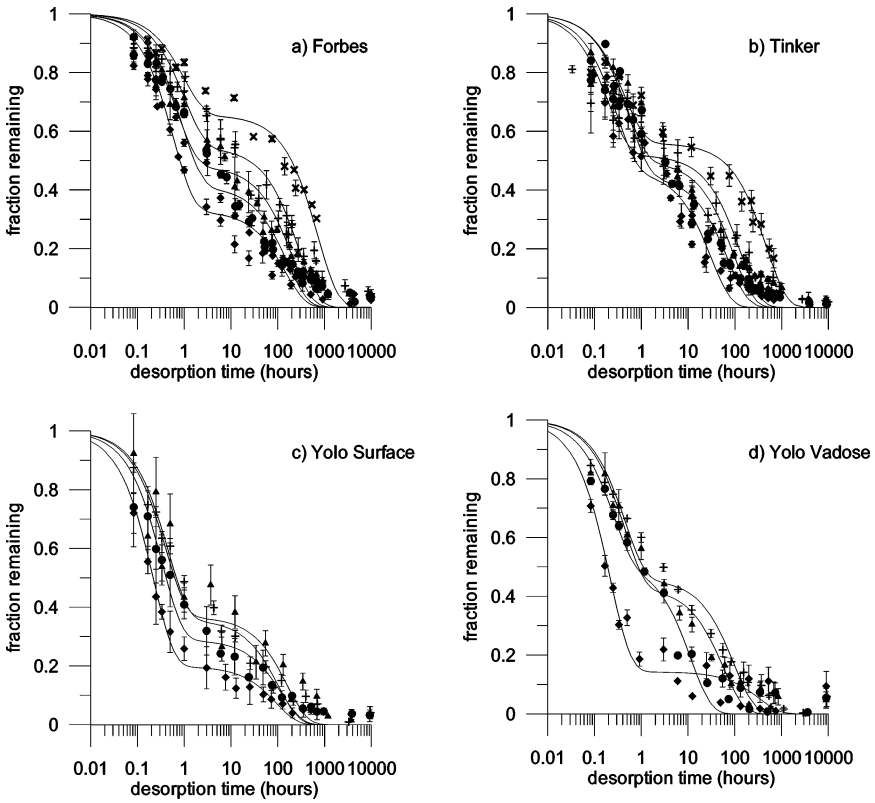

FIGURE 3. Desorption curves and the fit to the two-site model. Aging times: ◆, 1 h; ●, 1 day; ▲, 1 week; +, 1 month; ×, 18 months. Initial phenanthrene loading targets were Forbes 160 μg/g, Tinker 400 μg/g, Yolo Surface 48 μg/g, Yolo Vadose 24 μg/g. Error bars represent one standard deviation.

O-containing groups (O-containing heterocyclics, phenols, furans, aldehydes/ketones, alcohols, and acids). Component two, which accounts for 22.5% of the variation, is mainly carbon dioxide, benzene, condensed aromatics nitriles/amines, and N-containing heterocyclics. Component one is mainly of lignin and carbohydrate origin and component two is mainly of carbohydrate and protein origin although the origin of carbon dioxide is unknown. The first component effectively differentiates the Tinker soil from the rest while the second component differentiates the Forbes soil. Overall, Forbes and Tinker soils are distinctly different, while Yolo Surface and Yolo Vadose are different but closer to each other in composition as expected.

Phase Distribution Relationships. Phenanthrene sorption and desorption data for each soil were fit using the Freundlich model ($q_e = K_F C_e^n$) where q_e is the phenanthrene concentration in soil (μg/g), C_e is the aqueous phase concentration (μg/L), K_F is the Freundlich unit capacity factor (μg/kg)(μg/L)$^{-n}$, and n is the Freundlich exponent (Table 3). Both sorption and desorption PDRs for all four soils were nonlinear ($n < 1$ with 95% confidence interval; $p < 0.05$). Yolo Vadose had the greatest OC normalized distribution coefficients for sorption after 1 week (K_{OC} at C_e= 100 μg/L, see footnote to Table 3) followed by Tinker, Yolo Surface, and Forbes. For desorption, the K_{OC} values were in the order of Yolo Vadose > Forbes > Tinker > Yolo Surface. Literature values of K_{OC} for phenanthrene at $C_e = 100$ μg/L have been reported as 11.8−21.8 L/g for soils (*19*, *27*), 9.1−17.5 L/g for humic acids (*19*, *31*), 303−321 L/g for shale (*19*), and 411−599 L/g for kerogen (*19*).

The Hysteresis Index (*HI*, defined in the footnote to Table 3) provides a quantitative measure of the difference between adsorption and desorption PDRs (*56*). Literature values of *HI* for phenanthrene at $C_e = 100$ μg/L have been reported as 0.12−0.66 for soils and sediments (*57*), 0.153 and 0.183 for humic acids (*57*), 0.295−0.479 for coals (*57*), 0.484 for kerogen (*57*), 0.633−2.470 for synthetic polymers (*58*), and 0.11−0.30 for soil treated with subcritical water extraction (*27*). *HI* values for the soils tested in this study ranged from 0.080 (Tinker) to 0.75 (Yolo Vadose). *HI* values near zero (Tinker, Yolo Surface) suggest that the sorption process had reached equilibrium within the 1-week contact time for these

TABLE 4. Desorption Rate Two-Site Model Parameters

soil	aging time	f	k_f (h^{-1})	k_s (h^{-1})	correlation coefficient	N[a]	final concn ($\mu g/g$)[b]	final time[c] (hours)
Forbes	1 h	0.671	1.7	6.8E-3	0.983	124	2.9 (0.47)	9897
	1 d	0.588	1.1	6.1E-3	0.988	124	3.9 (1.25)	9959
	1 week	0.519	1.4	4.9E-3	0.983	120	4.1 (0.28)	9891
	1 month	0.455	0.96	3.6E-3	0.984	111	4.3 (0.90)	9941
	18 months	0.345	1.0	1.4E-3	0.981	48	29.7 (1.06)	678
Tinker	1 h	0.534	3.3	3.3E-2	0.984	118	4.5 (0.27)	9213
	1 d	0.552	1.8	1.4E-2	0.985	118	3.2 (0.71)	9266
	1 week	0.502	2.0	1.1E-2	0.980	114	7.6 (3.68)	9249
	1 month	0.480	5.0	7.7E-3	0.975	111	6.1 (1.76)	9407
	18 months	0.441	2.3	2.1E-3	0.976	48	46.8 (8.22)	671
Yolo Surface	1 h	0.802	4.5	1.1E-2	0.995	54	1.9 (1.29)	9243
	1 d	0.711	2.9	8.3E-3	0.989	60	2.0 (0.69)	9272
	1 week	0.633	2.5	6.3E-3	0.969	60	1.4 (0.48)	9214
	1 month	0.642	2.2	9.7E-3	0.992	57	2.2 (1.11)	9575
Yolo Vadose	1 h	0.857	4.6	3.0E-3	0.978	57	2.1 (1.18)	9049
	1 d	0.488	4.0	8.7E-2	0.991	57	1.0 (0.62)	9054
	1 week	0.572	2.3	1.7E-2	0.992	57	2.1 (1.68)	9009
	1 month	0.542	2.2	1.0E-2	0.991	60	1.2 (0.72)	9316

[a] N: number of data points. [b] () shows standard deviation. [c] Time when soil samples were freeze-dried.

materials. *HI* values were largest for Forbes and Yolo Vadose, in that sorption did not attain equilibrium during the allotted contact time.

Desorption Rate Studies. Desorption rates for the four soils following different phenanthrene aging periods are shown in Figure 3. Each set of data was fit to the two-site model ($F = f\exp(-k_f t) + (1 - f)\exp(-k_s t)$) where F is the fraction of phenanthrene remaining sorbed to the soil at time t, f is the fraction of sorbate exhibiting fast release rates, k_f is the rate constant for the fast fraction (h^{-1}), and k_s is the rate constant for the slow fraction (h^{-1}). The fit to the two-site model was relatively good with a minimum correlation coefficient of 0.969. The two-site model parameters and the final sorbed phase concentrations are summarized in Table 4 and the changes in the parameters with aging time are shown in Figure 4. The lines in Figure 4 are the fit of two-site model parameters to the power function or the logarithmic function as a function of the aging time.

Phenanthrene concentrations remaining in the soil after approximately 1 year of desorption were not significantly different between different aging periods for Tinker, Yolo Surface, and Yolo Vadose. The average residual phenanthrene concentrations for the 1 h, 1 d, 1 week, and 1 month aging times were 5.4 $\mu g/g$, 1.9 $\mu g/g$, and 1.6 $\mu g/g$ for Tinker, Yolo Surface and Yolo Vadose, respectively. Forbes soil showed an increase in the final concentration from 2.9 $\mu g/g$ after 1 h of aging time to 4.8 $\mu g/g$ after 1 month of aging time ($p < 0.1$). Kan et al. (*59*, *60*) and Chen et al. (*61*) observed that sediments reached a "maximum irreversible capacity" after a series of uptake and release cycles. The capacity was reported as 10−12 $\mu g/g$ (*59*), 0.34−134 $\mu g/g$ (*60*), and 0.45−271 $\mu g/g$ (*61*) depending on geosorbents and contaminants.

Literature values of f for hydrophobic organic compounds desorption from soils and sediments have been reported as 0.1−0.93 (*2*, *62*−*64*), for k_f as 0.001−0.5 (h^{-1}) (*2*, *63*, *64*), and for k_s as 3.6×10^{-5}−7.8×10^{-3} (h^{-1}) (*2*, *62*−*65*). These parameters are functions of types of geosorbent, aging time, and contaminant loading (*64*) and are subject to experimental duration especially for k_s (*66*). The parameters derived in this study were 0.35−0.86 (f), 0.96−5.0 h^{-1} (k_f), and 1.4×10^{-3}−8.7×10^{-2} h^{-1} (k_s). All of the k_f values and some of the k_s values from this study are greater than previously reported values. This may be caused by the spiking procedure. Aging times and contaminant loadings were comparable. In this study, phenanthrene was spiked as dichloromethane solution while in cited studies, contaminants were equilibrated with aqueous solutions either in the laboratory or in the field. Lu and Pignatello (*67*) suggested that DCM treatment (conditioning) causes structural changes in the SOM matrix, which can induce changes in sorption.

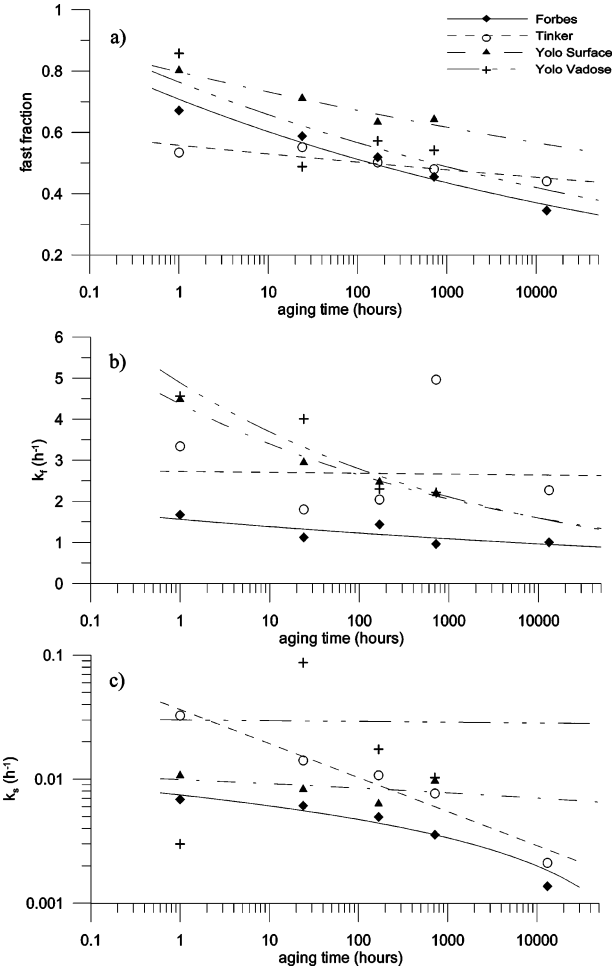

FIGURE 4. Two-site model parameters from the desorption rate experiment (a) fast fraction, (b) fast fraction rate constant, and (c) slow fraction rate constant. The lines are fit as a function of aging time. (a) Power function, (b) power function, (c) logarithmic function except for Tinker soil (power function).

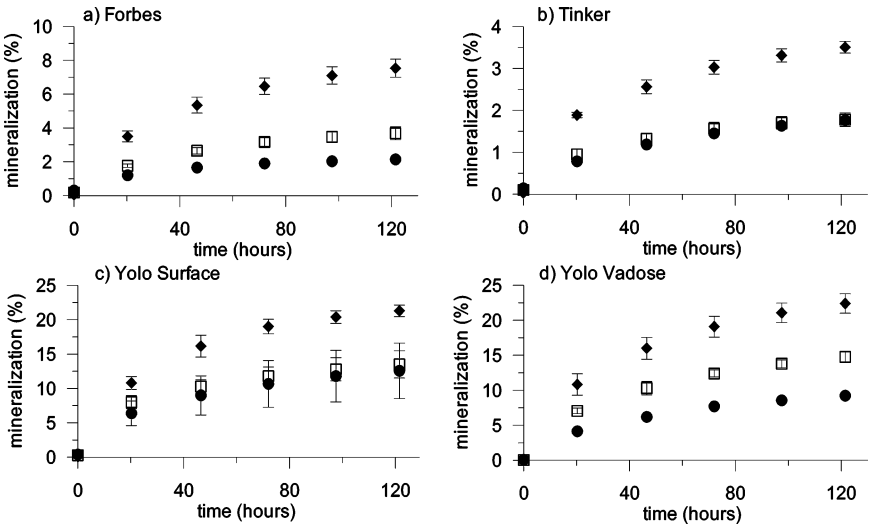

FIGURE 5. Cumulative mineralization of the four soils. ◆, 24 h; □, 168 h; ●, 600 h of aging. Error bars represent one standard deviation.

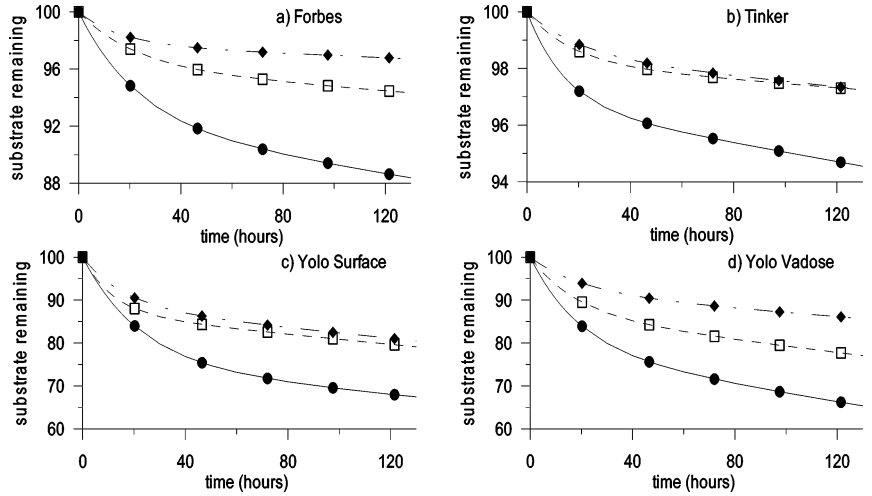

FIGURE 6. Bioadegradation curves and the fit to the two-site model. ◆, 24 h; □, 168 h; ●, 600 h of aging. Assumes that assimilation was 50% of mineralization.

TABLE 5. Bioavailability Two-Site Model Parameters

soil	aging time	*f*	k_f (h^{-1})	k_s (h^{-1})	R^2	N [a]
Forbes	24 h	0.078	4.3E-02	3.3E-04	0.9998	6
	168 h	0.038	4.6E-02	1.5E-04	0.9996	6
	600 h	0.023	6.1E-02	7.8E-05	0.9978	6
Tinker	24 h	0.033	6.8E-02	1.7E-04	0.9995	6
	168 h	0.018	5.8E-02	7.3E-05	0.9990	6
	600 h	0.015	4.9E-02	9.5E-05	0.9986	6
Yolo Surface	24 h	0.25	5.3E-02	1.5E-03	0.9998	6
	168 h	0.13	5.6E-02	9.3E-04	0.9997	6
	600 h	0.11	4.9E-02	5.4E-04	0.9995	6
Yolo Vadose	24 h	0.21	4.5E-02	8.4E-04	0.9998	6
	168 h	0.13	8.5E-02	7.3E-04	0.9996	6
	600 h	0.081	6.3E-02	7.4E-04	0.9996	6

[a] *N*: number of data points.

Mineralization Studies. Phenanthrene degraded slowest in Tinker soil for all aging times followed by Forbes soil (Figure 5). Yolo Surface and Yolo Vadose had similar degradation rates for the aging times of 24 h and 168 h; however, for the 600 h aging time, phenanthrene in Yolo Vadose degraded more slowly than in Yolo Surface. Increasing aging time from 24 h to 600 h decreased the amount of phenanthrene degraded and the maximum degradation rate. After 121.5 h of biodegradation, samples with 600 h of aging time degraded 28, 50, 59, and 41% less than the samples with 24 h of aging time for Forbes, Tinker, Yolo Surface, and Yolo Vadose, respectively. Similarly, the maximum degradation rate dropped by 26, 35, 47, and 38% from 24 h to 600 h of aging time for Forbes, Tinker, Yolo Surface, and Yolo Vadose, respectively. The fraction of phenanthrene remaining on the soil at each point during the mineralization studies was fitted to the two-site model (Figure 6, Table 5) with the assumption that two-thirds of the phenanthrene evolved as CO_2 and one-

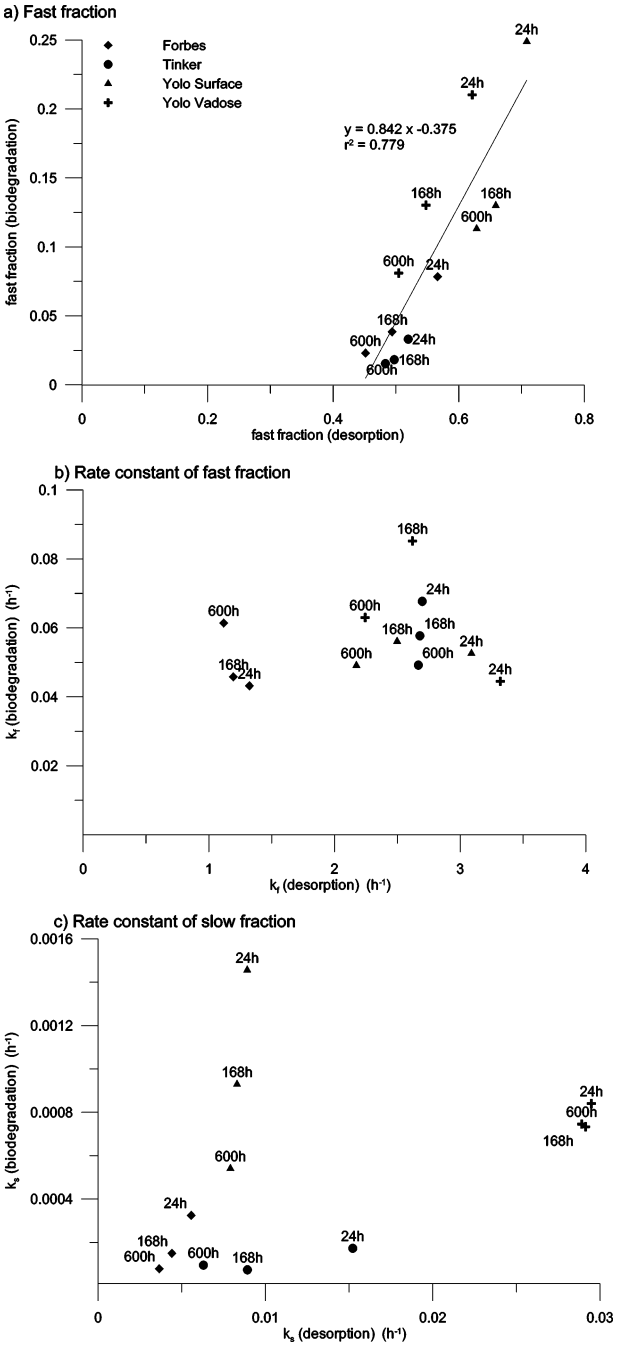

FIGURE 7. Relationships between the desorption rate experiment and the biodegradation experiment, (a) fast fraction, (b) rate constant of fast fraction, (c) rate constant of slow fraction. The desorption parameters in these figures are calculated from the fit in Figure 4, not the numbers derived in Figure 3, to allow comparison of the desorption and biodegradation rate parameters at the same aging times (24, 168, 600 h). The numbers next to data points indicate aging times.

third was assimilated into biomass (*39*). In biodegradation, the effect of increasing aging times appeared predominantly in the fast fraction f and the slow rate constant k_s.

Relation between Biodegradation and Desorption Rate. Abiotic sorption and desorption regulate the availability of contaminants to microorganisms in soil. Although there is evidence of microbiologically facilitated desorption (*8*, *41*, *68*), the majority of the sorbed portion of compounds does not appear to be degraded until the compound enters the solution phase. If desorption limits biodegradation rate, the following observations are expected.

(1) The fast fraction f derived from the mineralization studies should be related to that of the desorption studies. The fraction that is readily available for desorption should be readily available for bacteria to utilize as well.

(2) The slow rate constant k_s of the desorption studies is related to that of the mineralization studies. Biodegradation is expected to be limited by the rate of desorption primarily during the second slower stage of release.

The f values of desorption and biodegradation data show a linear relation ($p < 0.01$) across different soils and different aging periods (Figure 7 a) as hypothesized despite the fact that the two experiments were conducted in physical systems with different characteristics. The larger degree of mixing in the desorption experiments is expected to produce a larger fast fraction estimate than the less intensive mixing of the mineralization experiments; this may account for the large x-intercept in Figure 7a. Spatial heterogeneity of phenanthrene degrading bacteria in the experimental system may also contribute to limited mineralization. There was no significant relationship between the k_f values for desorption and the mineralization (Figure 7b). The k_f values for desorption were 2 orders of magnitude greater than those for biodegradation likely because of the more efficient mass transfer in the well-mixed desorption experiments. There also was no apparent correlation between the k_s values of desorption and biodegradation (Figure 7c).

The k_s values for desorption were 1 to 2 orders of magnitude greater than those for biodegradation for reasons outlined above. The k_s values for mineralization may be especially subject to error because of the short duration of the study (*66*).

The linear relationship between the f values for desorption and biodegradation supports the hypothesis that desorption limits biodegradation. However, the fast and slow rate constants for desorption and biodegradation did not show any significant relations. This inconsistency probably results from the differences in physical systems, and the experimental designs, which were necessitated by practical experimental considerations.

Structure/Function Relation. To test the hypothesis that there are SOM structures that cause desorption resistance, correlations were analyzed between soil characteristics and sorption/desorption and biodegradation parameters. Structural parameters employed in this analysis include the pyrolysis groups shown in Figure 1 and the principal components shown in Figure 2. In addition, free and amorphous iron and aluminum contents were included in the correlation analysis to test the hypothesis that the interactions between SOM and reactive iron/aluminum play a role in providing rigid and more resistant sorption sites. Functional parameters considered include K_{OC} and HI (sorption and desorption), maximum rate and extent of biodegradation, and two-site rate parameters f, k_f, k_s (desorption and biodegradation).

No statistically significant positive correlations were observed between the structural descriptors selected and the PDR derived functional parameters (K_{OC} and HI). Our experiments were thus not able to identify pyrolysis markers for SOM structures to which phenanthrene sorbs preferentially. The K_{OC} values negatively correlated with N-containing heterocyclics ($p < 0.05$). There have been limited attempts to relate K_{OC} values to pyrolysis structural information. Peuravuori (*69*) grouped the pyrolysis results of aquatic humic substances into likely precursors and observed that K_{OC} values of pyrene were negatively correlated with aliphatics and were positively correlated with nitrogen-containing polypeptides and proteins, the sum of phenol and methoxyphenols and other aromatics. Schultz et al. (*70*, *71*) found that K_{OC} values were positively correlated with hydrocarbon fragments and were negatively correlated with oxygen- and nitrogen-

TABLE 6. Correlations between Desorption Parameters and Pyrolysis Groups[a,b]

	parameters/aging time											
	f				k_f				k_s			
pyrolysis groups	1 h	1 d	1 week	1 month	1 h	1 d	1 week	1 month	1 h	1 d	1 week	1 month
alkanes	--											
alkenes	-	--	-									
benzene						-	--	--				
condensed aromatics					---	-						
O-containing heterocyclics	-											
N-containing heterocyclics										---	-	-
furans	--											
aldehydes/ketones	--											
alcohols	-											

[a] Positive correlations: +++, $p < 0.01$; ++, $p < 0.05$; +, $p < 0.10$. [b] Negative correlations: ---, $p < 0.01$; --, $p < 0.05$; -, $p < 0.10$.

TABLE 7. Correlations between Biodegradation Parameters and Pyrolysis Groups[a,b]

	parameters/aging time (h)														
	f			k_f			k_s			max rate			extent		
pyrolysis groups	24	168	600	24	168	600	24	168	600	24	168	600	24	168	600
alkanes													-		
alkenes	--	-	--				--	--		-	-	--	-	-	--
alkyl-substituted benzenes		-							--	-			-	--	
condensed aromatics									-						
O-containing heterocyclics				+											
N-containing heterocyclics					--										
phenols				++											
furans	-	-								-	-		--	-	
alcohols				+											
acids				+++											

[a] Positive correlations: +++, $p < 0.01$; ++, $p < 0.05$; +, $p < 0.10$. [b] Negative correlations: ---, $p < 0.01$; --, $p < 0.05$; -, $p < 0.10$.

containing fragments. It is difficult to compare these literature results directly to this study because pyrolysis results were quantified and presented differently. However, the inconsistency of correlations may suggest that these are not universally applicable descriptors of K_{OC} values. There have been numerous studies relating K_{OC} values to macroscopic SOM structures characterized by ^{13}C NMR. Various researchers proposed SOM descriptors including aromaticity (*24*, *72*, *73*), polarity (*23*), and both aromaticity and aliphaticity (*26*). Gunasekara et al. (*74*) concluded that no single macroscopic sorbent characteristic (e.g., aromaticity or aliphaticity) could account for K_{OC} variations. Similarly, simple characterization by pyrolysis may not be able to explain K_{OC} variations caused by the diversity of SOM. In addition, the finding may arise that pyrolysis GC-MS may not be the right tool to characterize the responsible SOM structures because only a small fraction of the SOM (e.g., hard carbon or black carbon) is responsible for high-capacity sorption and sequestration phenomena, and the characteristics of this pool are masked by the larger portion of OC with less diverse sorption behaviors.

There were statistically significant correlations between the K_{OC} values of desorption and the OC normalized concentrations of free iron ($p < 0.10$), free aluminum ($p < 0.05$), amorphous iron ($p < 0.05$), and between *HI* values and the OC normalized amorphous aluminum concentration ($p < 0.05$). There have been some investigations on the effect of underlying minerals on K_{OC} values. Murphy et al. (*29*) reported that the same humic substance on different minerals showed different K_{OC} values toward hydrophobic organic solutes. Onken and Traina (*30*) also formed humic acid−mineral complexes and showed that the K_{OC} values varied with organic matter content of the complex as well as with the identity of underlying minerals. Wang and Xing (*31*) also observed different K_{OC} values for the same humic acid on different clays. They also showed an increase in linearity with an increase of humic acid loading and suggested development of condensed structure as a result of close contacts between humic acid and mineral surface. Correlations in this study may support the hypothesis that reactive minerals influence the configuration and accessibility of SOM domains within soil, however, it is unclear why the K_{OC} values correlated with free iron, aluminum, and amorphous iron while the *HI* values only correlated with amorphous aluminum. Further investigations are necessary to study the interactions between minerals and soil organic matter and how/whether this interaction affects desorption resistance.

Statistically significant correlations ($p < 0.10$) are summarized in Tables 6 and 7 between pyrolysis groups and two-site model parameters of desorption and biodegradation, including maximum rate and extent of biodegradation. There was no consistent correlation between desorption and biodegradation parameters and free/amorphous iron and aluminum concentrations. The *f* values of desorption and biodegradation at shorter aging times showed negative correlations with aliphatic and O-containing pyrolysis markers. These pyrolysis marker groups may contribute to make the slow fraction more significant but only at shorter aging times. The k_f values of desorption showed negative correlations with benzene and condensed aromatics. The k_f values of biodegradation showed positive correlations with O-containing groups. Marker peaks that showed statistically significant correlations with the k_f values are different for desorption and biodegradation. The k_s values of desorption showed negative correlations with N-containing heterocyclics. The k_s values of bioavailability showed negative correlations with alkenes, alkyl substituted benzenes, and condensed aromatics. Maximum rate and extent of biodegradation negatively correlated with aliphatic groups, alkyl substituted benzenes, and furans. In general, correlations point to aliphatic (alkanes, alkenes, and alkyl-substituted

benzenes), lignin, and carbohydrate (O-containing heterocyclics, furans, aldehydes/ketones, alcohols, phenols, and acids) as possible descriptors with a significant limitation that it may only be valid at a shorter aging time (*75*).

Overall, correlations between functional (desorption/biodegradation) and structural (pyrolysis) descriptors were not strong. Possible reasons include the small range of natural organic matter types and number of soils in this study, the complexity of soil, and the limitations of pyrolysis GC-MS in characterizing the relevant structures. It may, for instance, fail to identify certain types of SOM such as charlike carbons. The high yield of OC as CO_2 and the possibility of side reactions in a pyrolysis chamber add uncertainty in the results.

Soil is a complex material with highly heterogeneous organic matter and minerals. Unlike synthetic or more homogeneous SOM precursor polymers, it is difficult to isolate structures that cause desorption resistance. A lack of strong correlations may suggest that multiple SOM structures engage collectively in creating desorption resistance, especially at longer aging times. Previous efforts to establish such correlations have included more diverse materials (e.g., shale (*71*), coal, kerogen, black carbon), and correlations may have been driven by such "end member" sorbents. SOM characteristics identified as influential may be one of many structures and the one that is identified may depend on the sorbent set studied.

One important result of this study, which includes extensive investigation of composition, sorption/desorption, and biodegradation for a limited number of soils, is to reemphasize the dependence of the factors that appear to control desorption and bioavailability limitations on the particular sample set studied. Various researchers have proposed diverse SOM descriptors on the basis of their own sets of soils and sediments; none of these descriptors are universally applicable, however, and several did not work for our sample set. Future sequestration research needs to include a wider range of soil samples and to more explicitly consider mineral/SOM interactions.

Acknowledgments

Funding for this research was provided by the National Science Foundation (BES9733621), the National Institute of Environmental Health Science (5P42 E.S.04699), the Department of Energy (DE-FG03-97ER62349), and the University of California Toxic Substances Research and Teaching Program. The views in this paper are those of the authors and do not necessarily represent the official views of the sponsoring organizations.

Supporting Information Available

Pyrograms of four soils, the list of the top 20 most abundant pyrolysis fragments and their carbon fractions, and sorption/desorption PDRs. This material is available free of charge via the Internet at http://pubs.acs.org.

Literature Cited

(1) Pignatello, J. J.; Ferrandino, F. J.; Huang, L. Q. Elution of Aged and Freshly Added Herbicides from a Soil. *Environ. Sci. Technol.* **1993**, *27*, 1563−1571.

(2) Cornelissen, G.; van Noort, P. C. M.; Govers, H. A. Desorption Kinetics of Chlorobenzenes, Polycyclic Aromatic Hydrocarbons, and Polychlorinated Biphenyls: Sediment Extraction with Tenax and Effects of Contact Time and Solute Hydrophobicity. *Environ. Toxicol. Chem.* **1997**, *16*, 1351−1357.

(3) Hatzinger, P. B.; Alexander, M. Effect of Aging of Chemicals in Soil on Their Biodegradability and Extractability. *Environ. Sci. Technol.* **1995**, *29*, 537−545.

(4) Northcott, G. L.; Jones, K. C. Partitioning, Extractability, and Formation of Nonextractable PAH Residues in Soil. 1. Compound Differences in Aging and Sequestration. *Environ. Sci. Technol.* **2001**, *35*, 1103−1110.

(5) Fu, M. H.; Mayton, H.; Alexander, M. Desorption and Biodegradation of Sorbed Styrene in Soil and Aquifer Solids. *Environ. Toxicol. Chem.* **1994**, *13*, 749−753.

(6) Scribner, S. L.; Benzing, T. R.; Sun, S.; Boyd, S. A. Desorption and Bioavailability of Aged Simazine Residues in Soil from a Continuous Corn Field. *J. Environ. Qual.* **1992**, *21*, 115−120.

(7) Kelsey, J. W.; Kottler, B. D.; Alexander, M. Selective Chemical Extractants to Predict Bioavailability of Soil-Aged Organic Chemicals. *Environ. Sci. Technol.* **1997**, *31*, 214−217.

(8) White, J. C.; Kelsey, J. W.; Hatzinger, P. B.; Alexander, M. Factors Affecting Sequestration and Bioavailabilty of Phenanthrene in Soils. *Environ. Toxicol. Chem.* **1997**, *16*, 2040−2045.

(9) Robertson, B. K.; Alexander, M. Sequestration of DDT and Dildrin in Soil: Disappearance of Acute Toxicity but Not the Compounds. *Environ. Toxicol. Chem.* **1998**, *17*, 1034−1039.

(10) Landrum, P. F.; Eadie, B. J.; Faust, W. R. Variation in the Bioavailability of Polycyclic Aromatic Hydrocarbons to the Amphipod Diporeia (SPP.) with Sediment Aging. *Environ. Toxicol. Chem.* **1992**, *11*, 1197−1208.

(11) Pignatello, J. J.; Xing, B. Mechanisms of Slow Sorption of Organic Chemicals to Natural Particles. *Environ. Sci. Technol.* **1996**, *30*, 1−11.

(12) Luthy, R. G.; Aiken, G. R.; Brusseau, M. L.; Cunningham, S. D.; Gshwend, P. M.; Pignatello, J. J.; Reinhard, M.; Traina, S. J.; Weber, W. J., Jr.; Westall, C. Sequestration of Hydrophobic Organic Contaminants by Geosorbents. *Environ. Sci. Technol.* **1997**, *31*, 3341−3347.

(13) Xing, B. S.; Pignatello, J. J. Dual-mode sorption of low-polarity compounds in glassy poly(vinyl chloride) and soil organic matter. *Environ. Sci. Technol.* **1997**, *31*, 792−799.

(14) Werth, C. J.; Reinhard, M. Effects of temperature on trichloroethylene desorption from silica gel and natural sediments. 2. Kinetics. *Environ. Sci. Technol.* **1997**, *31*, 697−703.

(15) Farrell, J.; Grassian, D.; Jones, M. Investigation of mechanisms contributing to slow desorption of hydrophobic organic compounds from mineral solids. *Environ. Sci. Technol.* **1999**, *33*, 1237−1243.

(16) Allen-King, R. M.; Grathwohl, P.; Ball, W. P. New modeling paradigms for the sorption of hydrophobic organic chemicals to heterogeneous carbonaceous matter in soils, sediments, and rocks. *Adv. Water Resour.* **2002**, *25*, 985−1016.

(17) Huang, W.; Peng, P.; Yu, Z.; Fu, J. Effects of organic matter heterogeneity on sorption and desorption of organic contaminants by soils and sediments. *Appl. Geochem.* **2003**, *18*, 955−972.

(18) Young, T. M.; Weber, W. J., Jr. A Distributed Reactivity Model for Sorption by Soils and Sediments. 3. Effects of Diagenetic Processes on Sorption Energetics. *Environ. Sci. Technol.* **1995**, *29*, 92−97.

(19) Huang, W.; Weber, W. J., Jr. A Distributed Reactivity Model for Sorption by Soils and Sediments. 10. Relationships between Desorption, Hysteresis, and the Chemical Characteristics of Organic Domains. *Environ. Sci. Technol.* **1997**, *31*, 2562−2569.

(20) Gustafsson, O.; Haghseta, F.; Macfarlane, J.; Gschwend, P. M. Quantification of the Dilute Sedimentary Soot Phase: Implications for PAH Speciation and Bioavailability. *Environ. Sci. Technol.* **1997**, *31*, 203−209.

(21) Accardi-Dey, A.; Gschwend, P. M. Assessing the combined roles of natural organic matter and black carbon as sorbents in sediments. *Environ. Sci. Technol.* **2002**, *36*, 21−29.

(22) Cornelissen, G.; Kukulska, Z.; Kalaitzidis, S.; Christanis, K.; Gustafsson, O. Relations between Environmental Black Carbon Sorption and Geochemical Sorbent Characteristics. *Environ. Sci. Technol.* **2004**, *38*, 3632−3640.

(23) Kile, D. E.; Wershaw, R. L.; Chiou, C. T. Correlation of Soil and Sediment Organic Matter Polarity to Aqueous Sorption of Nonionic Compounds. *Environ. Sci. Technol.* **1999**, *33*, 2053−2056.

(24) Chiou, C. T.; McGroddy, S. E.; Kile, D. E. Partition Characteristics of Polycyclic Aromatic Hydrocarbons on Soils and Sediments. *Environ. Sci. Technol.* **1998**, *32*, 264−269.

(25) Xing, B. S.; Chen, Z. Spectroscopic Evidence for Condensed Domains in Soil Organic Matter. *Soil Sci.* **1999**, *164*, 40−47.

(26) Chefetz, B.; Deshmukh, A. P.; Hatcher, P. G.; Guthrie, E. A. Pyrene Sorption by Natural Organic Matter. *Environ. Sci. Technol.* **2000**, *34*, 2925−2930.

(27) Johnson, M. D.; Huang, W.; Dang, Z.; Weber, W. J., Jr. A Distributed Reactivity Model for Sorption by Soils and Sediments. 12. Effects of Subcritical Water Extraction and Alternations of Soil Organic Matter on Sorption Equilibria. *Environ. Sci. Technol.* **1999**, *33*, 1657−1663.
(28) Johnson, M. D.; Huang, W.; Weber, W. J., Jr. A Distributed Reactivity Model for Sorption by Soils and Sediments. 13. Simulated Diagenesis of Natural Sediment Organic Matter and Its Impact on Sorption/Desorption Equilibria. *Environ. Sci. Technol.* **2001**, *35*.
(29) Murphy, E. M.; Zachara, J. M.; Smith, S. C. Influence of mineral-bound humic substances on the sorption of hydrophobic organic compounds. *Environ. Sci. Technol.* **1990**, *24*, 1507−1516.
(30) Onken, B. M.; Traina, S. J. The Sorption of Pyrene and Anthracene to Humic Acid-Mineral Complexes: Effect of Fractional Organic Carbon Content. *J. Environ. Qual.* **1997**, *26*, 126−132.
(31) Wang, K.; Xing, B. Structural and Sorption Characteristics of Adsorbed Humic Acid on Clay Minerals. *J. Environ. Qual.* **2005**, *34*, 342−349.
(32) Alexander, M. How Toxic Are Toxic-Chemicals in Soil. *Environ. Sci. Technol.* **1995**, *29*, 2713−2717.
(33) Zhang, W.; Bouwer, E.; Wilson, L.; Durant, N. Biotransformation of Aromatic Hydrocarbons in Subsurface Biofilms. *Water Sci. Technol.* **1995**, *31*, 1−15.
(34) Cornelissen, G.; Rigterink, H.; Ferdinandy, M. M. A.; Van Noort, P. C. Rapidly Desorbing Fractions of PAHs in Contaminated Sediments as a Predictor of the Extent of Bioremediation. *Environ. Sci. Technol.* **1998**, *32*, 966−970.
(35) White, J. C.; Hunter, M.; Nam, K.; Pignatello, J. J.; Alexander, M. Correlation between Biological and Physical Availabilities of Phenanthrene in Soils and Soil Humin in Aging Experiments. *Environ. Toxicol. Chem.* **1999**, *18*, 1720−1727.
(36) Ogram, A. V.; Jessup, R. E.; Ou, L. T.; Rao, P. S. C. Effects of Sorption on Biological Degradation Rates of (2,4-Dichlorophenoxy)acetic Acid in Soils. *Appl. Environ. Microbiol.* **1985**, *49*, 582−587.
(37) Scow, K. M.; Hutson, J. Effect of Diffusion and Sorption on the Kinetice of Biodegradation - Theoretical Considerations. *Soil Sci. Soc. Am. J.* **1992**, *56*, 119−127.
(38) Alvarez-Cohen, L.; McCarty, P. L.; Roberts, P. V. Sorption of Trichloroethylene onto a Zeolite Accompanied by Methanotrophic Biotransformation. *Environ. Sci. Technol.* **1993**, *27*, 2141−2148.
(39) Alexander, M. *Biodegradation and Bioremediation*, 2nd ed.; Academic Press: San Diego, CA, 1999.
(40) Tang, W.-C.; White, J. C.; Alexander, M. Utilization of Sorbed Compounds by Microorganisms specifically isolated for that purpose. *Appl. Microbiol. Biotechnol.* **1998**, *49*, 117−121.
(41) Guerin, W.; Boyd, S. A. Differential Bioavailability of Soil-Sorbed Naphthalene to Two Bacterial Species. *Appl. Environ. Microbiol.* **1992**, *58*, 1142−1152.
(42) Guerin, W.; Boyd, S. A. Bioavailability of Naphthalene Associated with Natural and Synthetic Sorbents. *Water Res.* **1997**, *31*, 1504−1512.
(43) Tang, J.; Carroquino, M. J.; Robertson, B. K.; Alexander, M. Combined Effect of Sequestration and Bioremediation in Reducing the Bioavailability of Polycyclic Aromatic Hydrocarbons in Soil. *Environ. Sci. Technol.* **1998**, *32*, 3586−3590.
(44) Bertsch, P. M.; Bloom, P. R. In *Part 3, Chemical methods*; Sparks, D. L., Page, A. L., Helmke, P. A., Loeppert, R. H., Soltanpour, P. N., Tabatabai, M. A., Johnson, C. T., Sumner, M. E., Eds.; SSSA, American Society of Agronomy: Madison, WI, 1996; pp 517−550.
(45) Loeppert, R. L.; Inskeep, W. P. In *Part 3, Chemical methods*; Sparks, D. L., Page, A. L., Helmke, P. A., Loeppert, R. H., Soltanpour, P. N., Tabatabai, M. A., Johnson, C. T., Sumner, M. E., Eds.; SSSA, American Society of Agronomy: Madison, WI, 1996; pp 639−664.
(46) Johnson, C. R. *Phenanthrene Biodegradation Kinetics in Soil*; University of California, Davis: Davis, CA, 1997.
(47) Loebmann, S. *Desorption Studies of Phenanthrene in Four Natural Soils Using Supercritical Carbon Dioxide*; University of California, Davis: Davis, CA, 2000.
(48) Weber, W. J.; Huang, W. L. A distributed reactivity model for sorption by soils and sediments. 4. Intraparticle heterogeneity and phase-distribution relationships under nonequilibrium conditions. *Environ. Sci. Technol.* **1996**, *30*, 881−888.
(49) Huang, W. L.; Weber, W. J. A distributed reactivity model for sorption by soils and sediments. 11. Slow concentration dependent sorption rates. *Environ. Sci. Technol.* **1998**, *32*, 3549−3555.
(50) Hinrichs, C. J. *Methods for Measuring Desorption Rates of Phenanthrene in Soil*; University of California, Davis: Davis, CA, 1999.
(51) Schwartz, E.; Scow, K. M. Using Biodegradation Kinetics to Measure Availability of Aged Phenanthrene to Bacteria Inoculated into Soil. *Environ. Toxicol. Chem.* **1999**, *18*, 1742−1746.
(52) Schwartz, E.; Trinh, S. V.; Scow, K. M. Impact of Methylene Chloride on Microorganisms and Phenanthrene Mineralization in Soil. *J. Environ. Qual.* **2002**, *31*, 144−149.
(53) Pignatello, J. J. Slowly Reversible Sorption of Aliphatic Halocarbons in Soils. 1. Formation of Residual Fractions. *Environ. Toxicol. Chem.* **1990**, *9*, 1107−1115.
(54) Schwartz, E.; Scow, K. M. Repeated Inoculation as a Strategy for the Remediation of Low Concentrations of Phenanthrene in Soil. *Biodegradation* **2001**, *12*, 201−207.
(55) Stevenson, F. J. *Humus Chemistry: Genesis, Composition, Reaction*; John Wiley & Sons: New York, 1994.
(56) Huang, W.; Hong, Y.; Weber, W. J., Jr. Hysteresis in the sorption and desorption of hydrophobic organic contaminants by soils and sediments 1. A comparative analysis of experimental protocols. *J. Contam. Hydrol.* **1998**, *31*, 129−148.
(57) Weber, W. J., Jr.; Huang, W.; Hong, Y. Hysteresis in the sorption and desorption of hydrophobic organic contaminants by soils and sediments 2. Effects of soil organic matter heterogeneity. *J. Environ. Qual.* **1998**, *31*, 149−165.
(58) Leboeuf, E. J.; Weber, W. J., Jr. Macromolecular Characteristics of Natural Organic Matter. 2. Sorption and Desorption Behavior. *Environ. Sci. Technol.* **2000**, *34*, 3632−3640.
(59) Kan, A. T.; Fu, G.; M., H.; Chen, W.; Ward, C. H.; Tomson, M. B. Irreversible Sorption of Neutral Hydrocarbons to Sediments: Experimental Observations and Model Predictions. *Environ. Sci. Technol.* **1997**, *32*, 8892−902.
(60) Kan, A. T.; Fu, G.; Hunter, M. A.; Tomson, M. B. Irreversible Adsorption of Naphthalene and Tetrachlorobiphenyl to Lula and Surrogate Sediments. *Environ. Sci. Technol.* **1998**, *31*, 22176−2185.
(61) Chen, W.; Kan, A. T.; Tomson, M. B. Irreversible Adsorption of Chlorinated Benzenes to Natural Sediments: Implications for Sediment Quality Criteria. *Environ. Sci. Technol.* **2000**, *34*, 385−392.
(62) Cornelissen, G.; van Noort, P. C.; Parsons, J. R.; Govers, H. A. J. Temperature Dependence of Slow Adsorption and Desorption Kinetics of Organic Compounds in Sediments. *Environ. Sci. Technol.* **1997**, *31*, 454−460.
(63) Cornelissen, G.; van Zuilen, H.; van Noort, P. C. M. Particle size dependence of slow desorption of in situ PAHs from sediments. *Chemosphere* **1999**, *38*, 2369−2380.
(64) Johnson, M. D.; Keinath, T. M., II.; Weber, W. J., Jr. A Distributed Reactivity Model for Sorption by Soils and Sediments. 14. Characterization and Modeling of Phenanthrene Desorption Rates. *Environ. Sci. Technol.* **2001**, *35*, 1688−1695.
(65) Carroll, K. M.; Harkness, M. R.; Bracco, A. A.; Balcarcel, R. R. Application of a Permeant/Polymer Diffusional Model to the desorption of Polychlorinated Biphenyls from Hudson River Sediments. *Environ. Sci. Technol.* **1994**, *28*, 253−258.
(66) Opdyke, D. R.; Loehr, R. C. Determination of Chemical Release Rates from Soils: Experimental Design. *Environ. Sci. Technol.* **1999**, *33*, 1193−1199.
(67) Lu, Y. F.; Pignatello, J. J. Demonstration of the "Conditioning effect" in soil organic matter in support of a pore deformation mechanism for sorption hysteresis. *Environ. Sci. Technol.* **2002**, *36*, 4553−4561.
(68) Calvillo, Y. M.; Alexander, M. Mechanisms of Microbial Utilization of Biphenyl Sorbed to Polyacrylic Beads. *Appl. Microbiol. Biotechnol.* **1996**, *45*, 383−390.
(69) Peuravuori, J. Binding of Pyrene on Lake Aquatic Humic Matter: the Role of Structural Descriptors. *Anal. Chim. Acta* **2001**, *429*, 75−89.
(70) Schultz, L. F.; Young, T. M.; Higashi, R. M. Sorption-desorption Behavior of Phenanthrene Elucidated by Pyrolysis-Gas Chromatography-Mass Spectrometry Studies of Soil Organic Matter. *Environ. Toxicol. Chem.* **1999**, *18*, 1710−1719.
(71) Schultz, L. F. *Sorption Environments and Mechanisms for Hydrophobic Organic Contaminants in Soil Organic Matter*; University of California at Davis: Davis, CA, 1999.
(72) Xing, B.; McGill, W. B.; Dudas, M. J. Cross-Correlation of Polarity Curves To Predict Partition Coefficients of Nonionic Organic Contaminants. *Environ. Sci. Technol.* **1994**, *24*, 1929−1933.
(73) Ahmad, R.; Kookana, R. S.; Alston, A. M.; Skjemstad, J. O. The Nature of Soil Organic Matter Affects Sorption of Pesticides. 1.

Relationships with Carbon Chemistry as Determined by 13C CPMAS NMR Spectroscopy *Environ. Sci. Technol.* **2001**, *35*, 878−884.

(74) Gunasekara, A. S.; Simpson, M. J.; Xing, B. Identification and Characterization of Sorption Domains in Soil Organic Matter Using Structurally Modified Humic Acids. *Environ. Sci. Technol.* **2003**, *37*, 852−858.

(75) Hatcher, P. G.; Dria, K. J.; Kim, S.; Frazier, S. W. Modern Analytical Studies of Humic Substances. *Soil Sci.* **2001**, *166*, 770−794.

Received for review December 9, 2004. Revised manuscript received April 7, 2005. Accepted May 27, 2005.

ES0480522